International Forum on Aeroelasticity and Structural Dynamics
IFASD 2024
17-21 June 2024, The Hague, The Netherlands

PRELIMINARY INVESTIGATION OF THE SUPERELASTIC MONOSTABLE SPOILER FOR DYNAMIC GUST LOADS ALLEVIATION

Andrea Castrichini[1], Enzo Cosentino[1], Federica Siotto[1], Xiaoyang Sun[1], Josh Coppin[1], Raul Lozano Vargas[1], Ignacio Ballesteros Ruiz[1], Michail Hadjipantelis[2]

[1]Airbus UK ltd.
Pegasus House Aerospace Avenue, BS34 7PA Filton, United Kingdon
andrea.a.castrichini@airbus.com

[2]University of Bath
Claverton Down, BA2 7AY Bath, United Kingdon

Keywords: Passive loads alleviation, gust loads, structural dynamics, composite structures

Abstract: This paper provides a preliminary investigation into the use of a novel passive aircraft flight loads alleviation device called the Superelastic Monostable Spoiler. The work focuses primarily on understanding the behaviour of such a device and the related loads alleviation performance during dynamic gust events. A number of different designed parameters is explored such as the trigger condition and the activation speed. The main aim of the paper is to define the preliminary operational requirements of such a device in order to guide the future detailed design which is here not addressed. It was found that the Superelastic Monostable Spoiler could potentially provide loads alleviation performance comparable with typical gust loads alleviation technologies currently used in modern civil aviation based on the use of ailerons and spoilers.

1 INTRODUCTION

As the global population and economic activities continue to expand, the aviation industry faces escalating pressure to address its environmental footprint since it currently contributes for approximately 2-3% of global carbon emissions and such a share is destined to rise with increasing flight volumes in the years to come. Therefore, pioneering sustainable aviation has become imperative in order to align with international climate goals and meet the growing societal demand for environmentally responsible travel.
Recent advancements in technology and policy have begun to pave the way for more sustainable aviation practices with the goal of achieving net zero emission by 2050 [1]. Such an ambitious goal is fraught with technological and engineering challenges and will be achieved via a number of strategic steps including: the progressive integration of sustainable aviation fuels (SAF); improved operational strategies such as optimized flight paths and air traffic management; the development of new fuel efficient aircraft design.
Aircraft flight and ground loads are the key elements in carrying out the aircraft structural sizing and therefore determining its weight. In order to minimise costs and fuel consumption, aircraft designers aim to achieve minimum structural weight, whilst ensuring that failure cannot occur at any point of an aircraft's operation and in-service life due to excessive stresses or deflections. Aircraft load alleviation strategies are of particular interest since they allow the mitigation of critical load cases thus preventing over sizing the structure.

Active loads alleviation devices have found an earlier development and application within the aeronautical industry with respect to passive approaches. The use of isotropic material (mostly aluminium alloys), standard wing structural elements (primarily spars with transverse ribs), fixed wing geometries (no morphing allowed) and a more conservative design approach, has led to build quite stiff aircraft structures enabling rather small deformations, which did not allow the exploitation of flexibility effects characterising the passive loads alleviation strategies. A thorough survey on the main milestones on the development of active systems is provided by Regan and Jutte [2] showing that aeroservoelastic effects can be exploited for a number of objectives ranging from the alleviation of peak gust and manoeuvre loads, mitigation of loads cycles to enhance the fatigue life, improvement of flight handling qualities, reduction and control of the structural deformation and flutter suppression. Forward and aft wing-tip vertical accelerometers, as well as fuselage vertical accelerometers and pitch gyroscopes were used to measure the bending and torsional wing motion together with the overall aircraft vertical displacement and pitch rotation. This information was used to control the deflection of the aerodynamic control surfaces in order to vary the wing lift distribution thus reducing the loads. Inner and outer spoilers as well as ailerons were deflected upward in order to reduce the wing lift for discrete gust and manoeuvre loads mitigation, whereas both an upward and downward deflections were allowed for flutter suppression and fatigue loads reduction during turbulence [3, 4].

Passive loads alleviation strategies are of particular interest since they would allow a mitigation of the aircraft loads without relying on active devices thus limiting the required activation power as well as the risks of failure cases. However, these kind of passive approaches exploit the fluid structure interaction effects to reduce the structural loads, therefore the performance may not be satisfactory for all the points of the flight envelope. An example of passive loads alleviation is given by aeroelastic tailoring that can be defined as ”the incorporation of directional stiffness into an aircraft structural design to control aeroelastic deformation, static or dynamic, in such a fashion as to affect the aerodynamic and structural performance of that aircraft in a beneficial way” [5, 6]. The basic idea behind aeroelastic tailoring consists of designing a wing structure that, when deformed under the action of external loads, generates an incremental aerodynamic loads distribution partially mitigating the structural loads. This is, in general, achieved through the coupling of the wing bending and torsional motions. A typical example is given by swept-back wings since the sweep angle introduces a geometric coupling between the bending and the pitching motions. Control and optimization of the bending torsion coupling can be also achieved through the use of anisotropic materials such as composite materials. A number of research activities have proposed the optimization of the stacking sequence of composite material layers with different thickness and fibres orientation in order to achieve the desired stiffness tailoring [5,6]. More recently Stodieck et al. have also investigated the use of tow-steered composites, consisting in laminates with variable angle tow plies allowing curvilinear fibres path and thus a continuous stiffness variation within each ply [7].

Similar coupling effects can be also allowed by the use of innovative structural shapes and arrangements, a number of works [8–10] have showed how aeroelastic tailoring effects can be enhanced by using curvilinear spar and rib elements or by varying the spar/ribs orientation along the wing span both for static and dynamic applications.

A recent consideration in aircraft design is the use of novel configurations, such as the NASA and Boeing truss-braced wing aircraft concept [11–13], always with the aim on enabling an improvement of the aerodynamic efficiency with a limited repercussion on the structural weight.

This paper investigates a novel load alleviation technology called Superelastic Monostable Spoiler (SMS) [14] recently studied by Wheatcroft et al [15] who proposed a structural arrangement characterised by sequential instabilities in order to achieve a passively actuated pop-up

spoiler type of system. The main idea consist in having a chain of buckling prone elements that would snap under the compression load induced by the wing motion during a gust or a manoeuvrer. The chain of structural instabilities is exploited in order to activate a pop-up spoiler which itself would lead to local flow separation with a consequent reduction of the local lift [16, 17]. If properly sized, the SMS would enable the pop-up spoiler actuation only when the local structural strain are higher than a specific threshold, thus enabling the deployment only for high loads event while keeping the spoiler stowed under normal cruise condition.
This work presents a preliminary investigation of the use of the SMS for dynamic loads reduction. The study focuses on the dynamic behaviour of the spoiler during gust induced actuation and retraction cycles and the related impact on the overall wing loads. A number o trade studies are presented looking at different SMS activation thresholds and spoiler deflection rate. This paper does not deal with the detailed structural and mechanical design of the SMS which will be addressed in future works. The reported results show promising gust loads alleviation capability.

2 MATHEMATICAL MODELLING

A representative civil aviation model is used for this work. The structure is modelled via a linear finite element model with lumped masses and the aerodynamic forces determined using the doublet lattice panel method [18]. Aerodynamic correction are also introduced in order to account for the correct lift and pitch moment distribution along the wing.
The dynamic equation of motion can be described in the time domain as follow

$$\bar{M}\ddot{\xi} + \bar{D}\dot{\xi} + \bar{K}\xi + \bar{C}_{\xi}^{T}\lambda = \bar{F}_{Aero} \tag{1}$$

where $\bar{M}$, $\bar{D}$ and $\bar{K}$ are the generalized mass damping and stiffness matrices respectively. The generalised aerodynamic forces are defined in the frequency domain as

$$\tilde{F}_{Aero} = q_{dyn}[Q(M_{ach}, k)\tilde{\xi} + Q_g(M_{ach}, k)\tilde{w} + Q_x(M_{ach})\tilde{\delta} + Q_{LAF}(M_{ach})\tilde{\sigma}] \tag{2}$$

where Q $(N_{Modes} \times N_{Modes})$, Q_g $(N_{Modes} \times N_{Panels})$, Q_x $(N_{Modes} \times N_{ControlSurf})$ and Q_{LAF} $(N_{Modes} \times 1)$ are respectively the generalized aerodynamic forces matrices related to the Fourier Transform of the generalized coordinates $\tilde{\xi}$, gust vector $\tilde{w}$, control surfaces vector $\tilde{\delta}$ and spoiler deflection $\tilde{\sigma}$ whereas $q_{dyn} = \frac{1}{2}\rho U_{\infty}^{2}$ is the dynamic pressure.
The aerodynamic matrices Q and Q_g were computed for a limited number of reduced frequencies $k = \frac{\omega c}{2U_{\infty}}$ (where c is the reference chord and U_{∞} the flight speed) and at a given Mach number. To allow for simulation in the time domain, the aerodynamic matrices were approximated, in the frequency domain, using the rational fraction approximation method proposed by Roger [19]. Following some manipulation, the aerodynamic loads can be formulated in the time domain as

$$\begin{aligned} \bar{F}_{aero} = q_{dyn}\Bigg\{ & \left[Q_0\xi + Q_1\frac{c}{2U_{\infty}}\dot{\xi} + Q_2\left(\frac{c}{2U_{\infty}}\right)^2\ddot{\xi}\right] \\ + & \left[Q_{g0}w + Q_{g1}\frac{c}{2U_{\infty}}\dot{w} + Q_{g2}\left(\frac{c}{2U_{\infty}}\right)^2\ddot{w}\right] \\ & + Q_x\delta + Q_{LAF}\sigma + \sum_{l=1}^{N_{Poles}} R_l \Bigg\} \end{aligned} \tag{3}$$

where R_l $(N_{Modes} \times 1)$ is the generic aerodynamic state vector related to the generic lag-pole $b_l = k_{max}/l$. These extra states allow the modelling of the unsteady aerodynamics by taking into account of the delay of the aerodynamic forces with respect to the structural deformations. These aerodynamic states are evaluated through the set of dynamic equations

$$\dot{R}_l = -b_l \frac{2U_\infty}{c} I R_l + Q^{\xi}_{2+l}\dot{\xi} + Q^{w}_{g2+l}\dot{w} \qquad l = 1 \cdots N_{Poles} \tag{4}$$

It is important to point out that only unsteady aerodynamic effect due to the structural deformation and the gust the unsteady aerodynamic effects are taken into account, whereas the aerodynamic forces due to the control surface and the SMS deflection are assumed to be quasi steady. Future work will focus on the modelling of the unsteady spoiler aerodynamic forces based upon the experimental works from Hadjipantelis et al. [16]. The generalised incremental aerodynamic forces due to a unitary SMS deployment, $Q_{LAF}(M_{ach})$, are computed by correcting the doublet lattice aerodynamics according to reference incremental wing lift and pitching moment values computed via a rigid and steady CFD calculation with the spoiler fully deployed. The evolution of the SMS induced aerodynamic forces during the passive extension and retraction is modelled as

$$F_{LAF} = Q_{LAF}\sigma(t) = Q_{LAF}\sigma_{ref}\phi(t) \tag{5}$$

Where σ_{ref} is the spoiler reference deflection for which the aerodynamic data have been computed and $\phi(t)$ is a linear ramp function that scales the spoiler deflection and as a consequence the related incremental aerodynamic contribution. Such a ramp up function is defined as follows during the spoiler extension

$$\begin{cases} \phi = 0. & if \quad t < t_{trigger} \\ 0 \leq \phi \leq \pm 1. & if \quad t_{trigger} \leq t \leq t_{trigger} + \Delta T_{deployment} \\ \phi = \pm 1. & if \quad t > t_{trigger} + \Delta T_{deployment} \end{cases}$$

whereas for a retraction it is defined as

$$\begin{cases} \phi = \pm 1 & if \quad t < t_{trigger} \\ \pm 1 \leq \phi \leq 0. & if \quad t_{trigger} \leq t \leq t_{trigger} + \Delta T_{deployment} \\ \phi = 0. & if \quad t > t_{trigger} + \Delta T_{deployment} \end{cases}$$

where the $\pm$ distinguish between a spoiler on the upper wing surface (producing negative aerodynamic incremental forces when deployed), for which a $+$ sign is considered, and a spoiler located on the lower wing surface (producing positive aerodynamic incremental forces) for which a $-$ is assumed. In this work the SMS is assumed to be placed in the outer part of the wing, with a position and span-wise lenght comparable with the standard dimension of a typical aileron.

3 NUMERICAL RESULTS

This paper focuses on analysing the SMS loads alleviation performance during gust conditions only since it is assumed that such a technology would definitively provide good manoeuvrer

loads alleviation capability. The exam question is whether a passively actuated device would be capable of providing satisfactory loads alleviation performance during a dynamic event for which the timing and reactivity of the movable is essential.
The dynamic gust response analyses are performed starting from a trimmed “1-g” flight configuration since the SMS deployment is driven by the total loaded status of the structure and not just by the dynamic increment.
Several gust response analyses were made assuming a ”1-cosine” gust profile over a range of gust lengths, between 18 m and 214 m, and intensities according to the European Aviation Safety Agency (EASA) Regulation [20] as well as a continuos turbulence gust case derived from real flight test measurements. Three mass cases were considered ranging from a Operative Weight Empty (OWE) to Maximum Take Off Weight (MTOW) cases as well as four flight points along the cruise speed curve from sea level to the cruise altitude.
The finite element model used for the investigation is representative of the global aircraft dynamics, however it is not suitable to accurately represent local stress distribution. Therefore, an approximation is introduce with respect to the SMS trigger logic which is that the SMS is deployed and retracted based upon the local wing-tip displacement with respect to the wing root and not the local wing-tip strain. Despite the two quantities show a degree of correlation, it is this latter that in reality would determine the SMS behaviour. Nevertheless, given the preliminary nature of this study, monitor the wing-tip displacement was assumed to be a reasonable assumption that would not change the qualitative finding of this work.
All the reported results have been normalised as follow

- The bending moments values are normalised with respect to the wing root bending moment limit load (LL)
- The non-dimensional time is normalised with respect to the first wing bending moment frequency as $\tau = t * f_{1^{st} Wing Bending Mode}$
- The wing span-wise position is normalised against the wing semi-span

For every case the SMS loads alleviation performance is compared with respect to a baseline model with no Loads Alleviation Function (LAF) and a model where the SMS is deployed in a similar manner of a typical LAF based upon actuated movables: after the gust is detected based upon sensors such as alpha vanes or accelerometers, a signal is sent to the movable in order to command its deployment; the movable is deployed at a certain speed in line with modern actuator performance and kept deflected at a constant angle during the entire loads event. Such a comparison allow to assess the SMS LAF performance with respect to a movable that produces the same aerodynamic incremental forces but it is actively actuated.
Since the SMS is a passive loads alleviation device, it is expected that its loads alleviation capabilities would not to be as good as typical LAF strategies. Due to the sudden and dynamic nature of a gust encounter, effective gust alleviation technologies requires the capability to detect the gust and deploy the LAF related control surface as quickly as possible with the goal of developing gust adverse incremental aerodynamic forces before the gust produces the peak wing loads. On the other hand, the SMS is actuated by the gust induced wing strain therefore, it is expected that its deployment might occur when the gust has already produce the maximum loads at the wing root. This is particularly true for a modern civil aircraft with swept back wing for which a SMS located close to the wing-tip would experience gust induced strain, and so deploy, after the gust has already gone past the majority of the wing.

Figure 1 reports the wing bending moment envelope due to the different load cases considered as well as the time histories of the wing root bending moment and the related spoiler deployment

for a single flight, point mass case and gust lenght. The spoiler deployment plot shows curves that can evolve linearly between the value of 0 if un-deployed and 1 when fully deployed. A number of different wig-tip displacement thresholds are investigate from 40% to 52% Limit Loads (LL) displacements. The SMS is assumed to deploy [retract] as soon as the wing-tip goes above [below] the selected displacement threshold. The spoiler deployment and retraction speeds are assumed to be the same kept constant for all the cases.
The results show that the lower the threshold value, the earlier the spoiler deploys, hence better the loads alleviation. For the lower wing-tip displacement thresholds, the spoiler exhibits better loads alleviation when compared against the typical actuated LAF, whereas little to none loads alleviation is observed for the higher threshold values. As expected, for the higher actuation threshold the spoiler deploys too late and it does not have enough time to counteract the gust induced loads especially at the wing root. Moreover, differently from the typical actuated LAF, the SMS does not increase the negative loads with respect to the baseline model since the tend to retract before the gust induced negative peak loads occur. Undesired post gust SMS-induced wing oscillations are observed for the lower actuation thresholds. This is due to the fact that, after the dynamic gust event, the wing tends to oscillate around the actuation threshold value (which for the lower cases is just above the 1g level) hence leading to undesired spoiler deployment and retraction, leading to further wing oscillation and spoiler activation.

Figure 2 reports a similar investigation but this time for number of different deployment and retraction speeds. For all the cases the SMS is assumed to deploy [retract] as soon as the wing-tip exceeds [goes below] 42% LL displacement. Deployment and retraction speeds are assumed to be the same.
The results show that the faster is the spoiler deployment speed better the loads alleviation performance. For the lower deployment speeds, the spoiler exhibits better loads alleviation when compared against the actuated LAF, whereas for the lower actuation speeds little to no loads alleviation is observed. However, it is also observed that a quick spoiler deployment produces an initial loads increment due to the impulsive inertia loads generated by the sudden dynamics. Also in this case undesired self induced wing oscillation are observed for the activation speeds.

Figure 3 show the same study as in the previous case, but this time for a continuos turbulence gust. In this case, very poor loads alleviation performance is observed for the SMS regardless how quickly it is actuated. For some cases the SMS even leads to higher loads when compared against the baseline model thus leading to increase the loads instead of alleviating them. Such unexpected behaviour can be understood looking at the time histories of the wing root bending moment and spoiler deployment in fig. 3. Every time the spoiler deploys it generates a negative incremental aerodynamic loads that pushes the wing downwards. Thus the wing absorbs elastic energy that gets released as soon as the spoiler goes back in its stowed configuration. The wing will then swing back upward with more emphasis than it would have done otherwise leading to a higher positive loads as well as upward wing bending deflection which in turn activates the spoiler again. Despite the SMS successfully reduce the first gust induced peak loads, it can be concluded that in a continuos turbulence, the repeated spoiler deflection and retraction can tune with the wing bending dynamic and lead to an amplification of the wing oscillation and loads.

Such an undesired effect can be mitigated by preventing the SMS to excite the wing bending mode while still counteracting the gust induced loads. A possible solution could be the design of a SMS that exhibits different wing-tip displacement thresholds and/or different speeds between deployment and retraction.
Figure 4 shows a study where the deployment and retraction speed is kept constant, the SMS

is assumed to deploy at 42% LL displacement while the retraction threshold is varied between 40% and 10% LL displacements. It is shown that, for the range of values considered, lowering the retraction threshold has little impact on the undesired SMS induced wing dynamics and loads. It is important also to point out that a very low or even negative retraction threshold would also increase the risk of the SMS to remain deployed after the gust event with a negative impact in the aerodynamic drag and fuel burn performance.
An alternative strategy could be to allow much slower retraction speeds in order to mitigate the wing upward swing after the spoiler retraction. A study is reported in Fig. 5 for different spoiler retraction rates while the spoiler actuation threshold and deployment speeds are fixed. The results shows indeed that the slower the spoiler retraction, the less the SMS induced wing oscillation and the better the loads alleviation performance.

4 CONCLUSIONS

This paper has provided a preliminary investigation into the use of the Super Elastic Monostable Spoiler for passive gust loads alleviation device. The work focused mainly in understanding the dynamic behaviour of such a device and how it would influence the wing loads during dynamic gust cases.
A number of studies have been introduced by varying the spoiler deployment and retraction speed as well as activation/retraction thresholds. It was shown that the SMS can provide similar loads alleviation capabilities compared with standard LAF strategy. The best performance have been observed when the SMS deploys as early and as quickly as possible while retracting slowly in order to avoid undesired self induced wing dynamic vibration.
Future study should consider different spoiler dimensions, numbers as well as locations, both span-wise, chord-wise and upper and lower surface in order to identify the optimum spoiler architecture. The modelling of unsteady aerodynamic effects induced by the spoiler activation should also be accounted for. Finally a more representative finite element model should be used in order to allow a deployment and retraction modelling based upon the local strain and not the global wing-tip displacement.

5 REFERENCES

[1] Group, A. T. A. (2021). Waypoint 2050.

[2] Regan, C. and Jutte, C. (2012). Survey of applications of active control technology for gust alleviation and new challenges for lighter-weight aircraft. Tech. rep.

[3] Karpel, M. (1981). Design for active and passive flutter suppression and gust alleviation. Tech. rep.

[4] Norman, D. (1981). Practical gust load alleviation and flutter suppression control laws based on a lqg methodology. Tech. rep.

[5] Weisshaar, T. A. (1981). Aeroelastic tailoring of forward swept composite wings. *Journal of Aircraft*, 18(8), 669–676.

[6] WEISSHAAR, T. (1987). Aeroelastic tailoring-creative uses of unusual materials. In *28th Structures, Structural Dynamics and Materials Conference*. p. 976.

[7] Stodieck, O., Cooper, J. E., Weaver, P., et al. (2015). Optimization of tow-steered composite wing laminates for aeroelastic tailoring. *AIAA Journal*, 53(8), 2203–2215.

[8] Locatelli, D., Mulani, S. B., and Kapania, R. K. (2011). Wing-box weight optimization using curvilinear spars and ribs (sparibs). *Journal of Aircraft*, 48(5), 1671–1684.

[9] Abdelkader, A., Harmin, M., Cooper, J., et al. (2011). Aeroelastic tailoring of metallic wing structures. In *52nd AIAA/ASME/ASCE/AHS/ASC Structures, Structural Dynamics and Materials Conference 19th AIAA/ASME/AHS Adaptive Structures Conference 13t*. p. 1712.

[10] Francois, G., Cooper, J. E., and Weaver, P. (2016). Impact of the wing sweep angle and rib orientation on wing structural response for un-tapered wings. In *57th AIAA/ASCE/AHS/ASC Structures, Structural Dynamics, and Materials Conference*. p. 0472.

[11] Nguyen, N. T., Ting, E., and Lebofsky, S. (2015). Aeroelasticity of axially loaded aerodynamic structures for truss-braced wing aircraft. In *56th AIAA/ASCE/AHS/ASC Structures, Structural Dynamics, and Materials Conference*. p. 1840.

[12] Zhao, W., Kapania, R. K., Schetz, J. A., et al. (2015). Nonlinear aeroelastic analysis of sugar truss-braced wing (tbw) wind-tunnel model (wtm) under in-plane loads. In *56th AIAA/ASCE/AHS/ASC Structures, Structural Dynamics, and Materials Conference*. p. 1173.

[13] Chen, P.-C., Zhou, Z., Ghoman, S. S., et al. (2015). Low-weight low-drag truss-braced wing design using variable camber continuous trailing edge flaps. In *56th AIAA/ASCE/AHS/ASC Structures, Structural Dynamics, and Materials Conference*. p. 1176.

[14] Cosentino, E. and Llewellyn-Jones, C. R. (2020). Flow control device.

[15] Wheatcroft, E., Shen, J., Groh, R., et al. (2023). Structural function from sequential, interacting elastic instabilities. *Proceedings of the Royal Society A*, 479(2272), 20220861.

[16] Hadjipantelis, M., Son, O., Wang, Z., et al. (2024). Frequency response of separated flows on a plunging finite wing with spoilers. *Experiments in Fluids*, 65(3), 36.

[17] Heathcote, D. J., Gursul, I., and Cleaver, D. (2018). Aerodynamic load alleviation using minitabs. *Journal of Aircraft*, 55(5), 2068–2077.

[18] Albano, E. and Rodden, W. P. (1969). A doublet-lattice method for calculating lift distributions on oscillating surfaces in subsonic flows. *AIAA journal*, 7(2), 279–285.

[19] Roger, K. L. (1977). Airplane math modeling methods for active control design.

[20] EASA (2007). Certification specifications for large aeroplanes cs-25.

COPYRIGHT STATEMENT

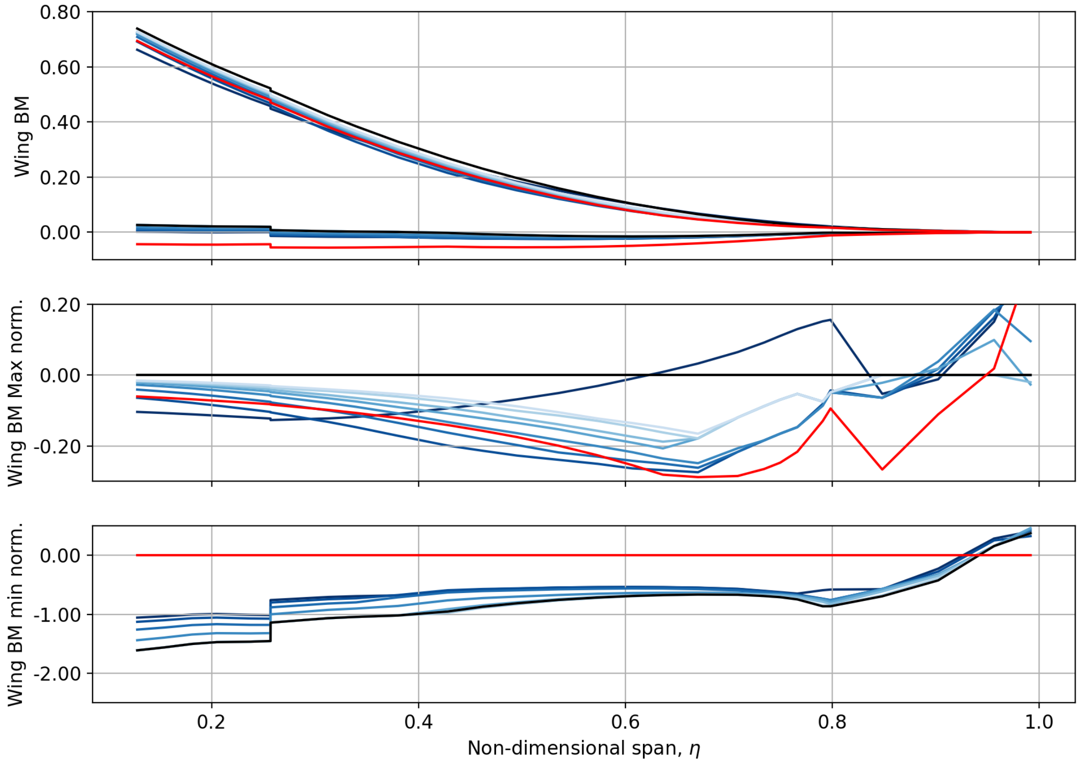

(a) Wing bending moment distribution - gust loads envelope

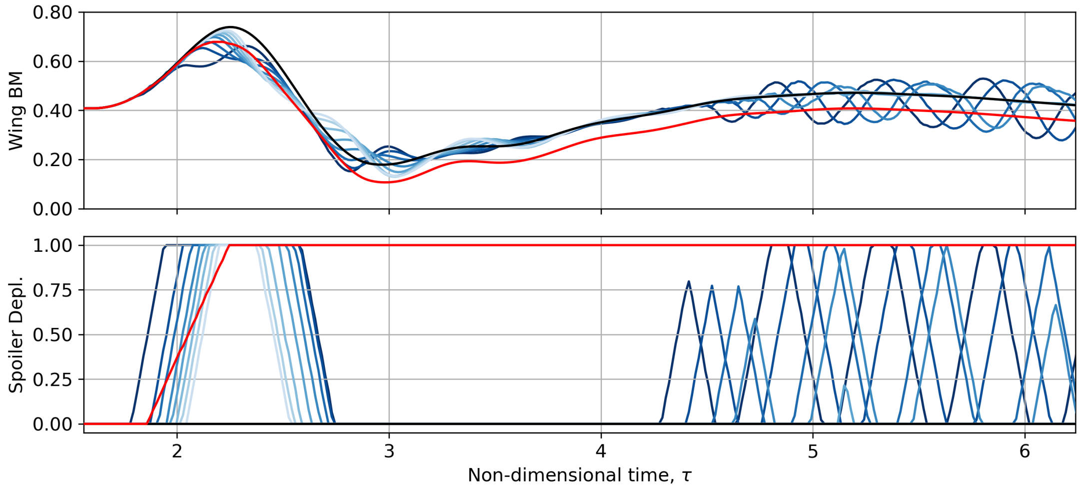

(b) Wing root bending moment and spoiler deflection time histories for a ”1-cosine” gust

Figure 1: SMS dynamic response for different wing-tip displacement thresholds
(—: baseline model with no LAF; —: actuated LAF;
—(from dark to light): SMS for different wing-tip displacement thresholds)

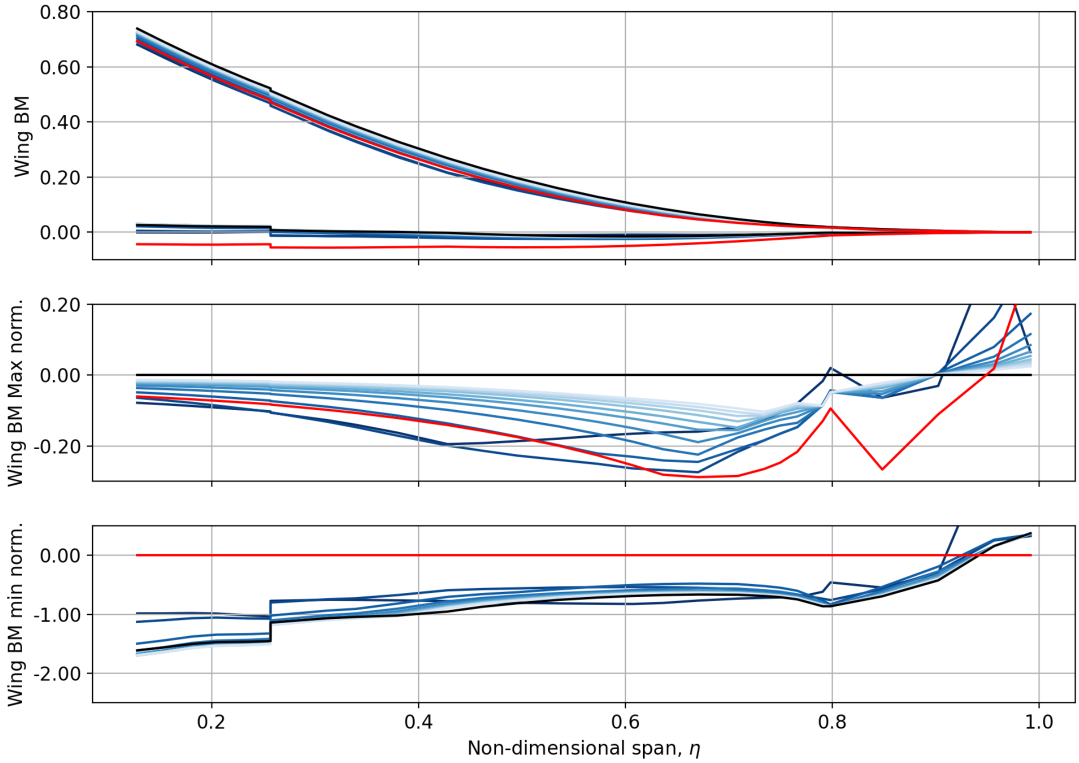

(a) Wing bending moment distribution - gust loads envelope

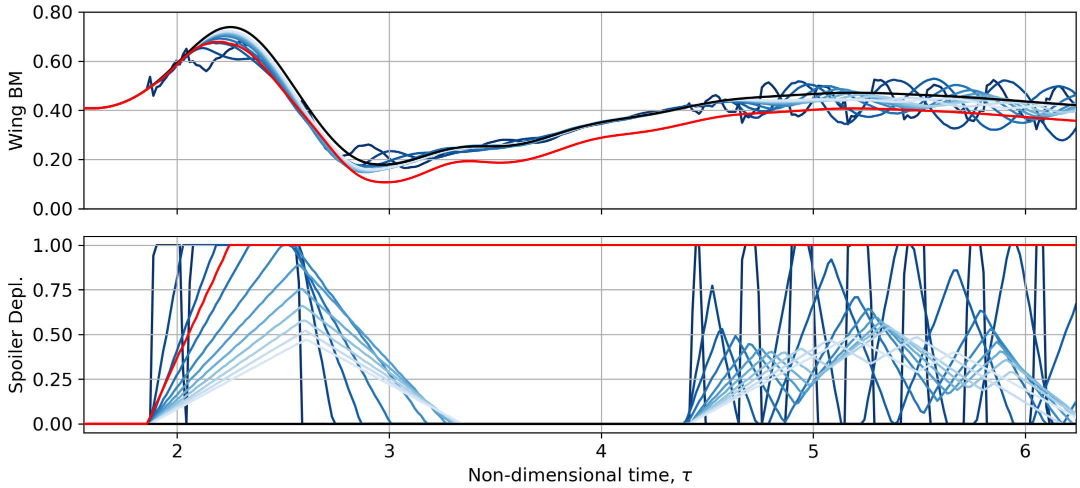

(b) Wing root bending moment and spoiler deflection time histories for a "1-cosine" gust

Figure 2: SMS dynamic response for different deployment and retraction speeds
(—: baseline model with no LAF; —: actuated LAF;
—(from dark to light): SMS for different deployment and retraction speeds)

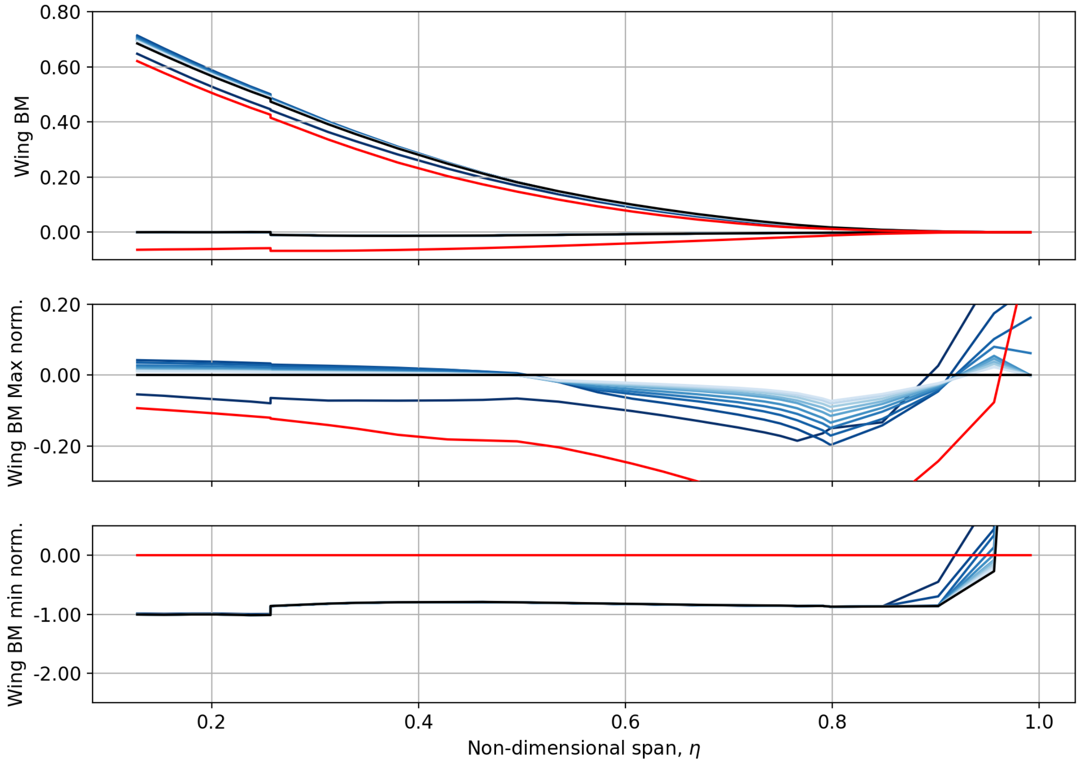

(a) Wing bending moment distribution - gust loads envelope

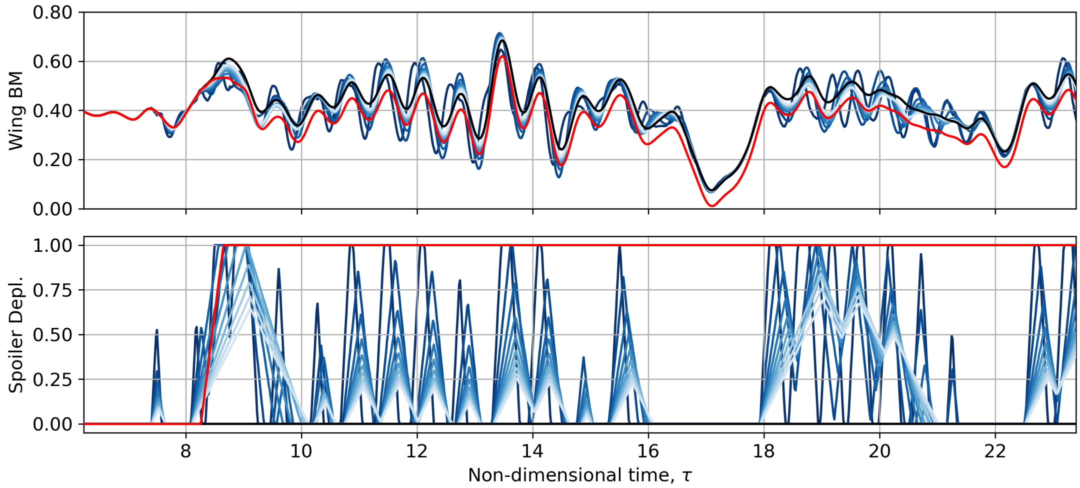

(b) Wing root bending moment and spoiler deflection time histories for a continuos turbulence gust

Figure 3: SMS dynamic response for different deployment and retraction speeds
(—: baseline model with no LAF; —: actuated LAF;
—(from dark to light): SMS for different deployment and retraction speeds)

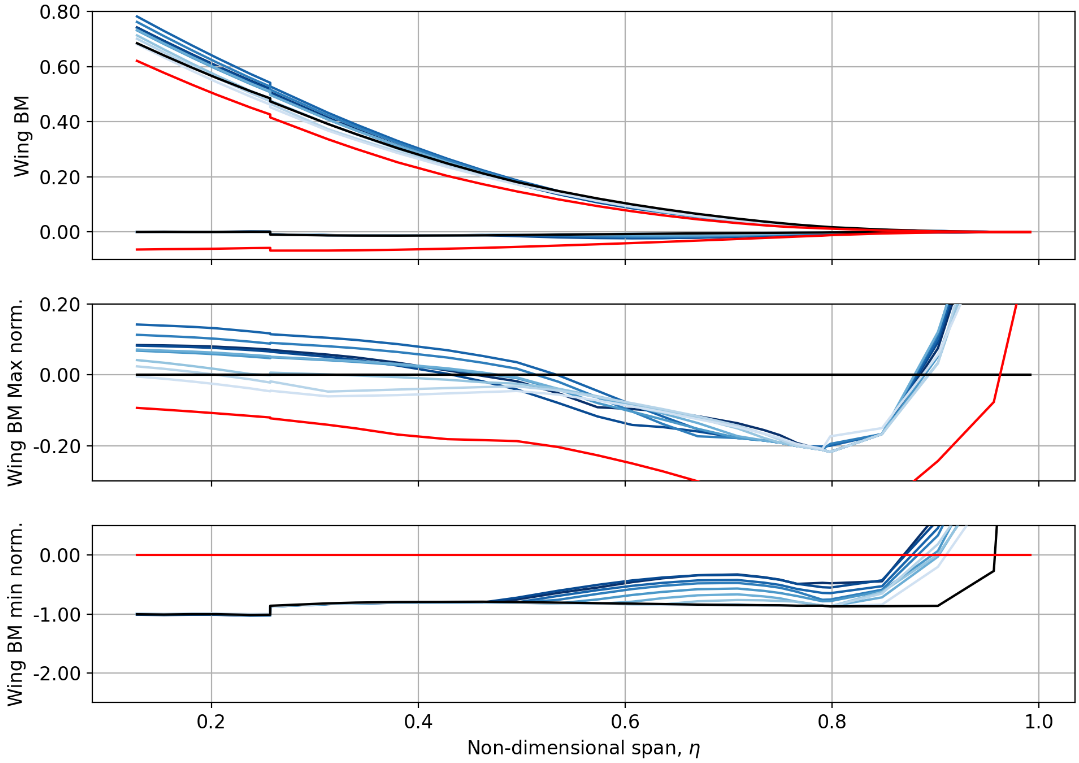

(a) Wing bending moment distribution - gust loads envelope

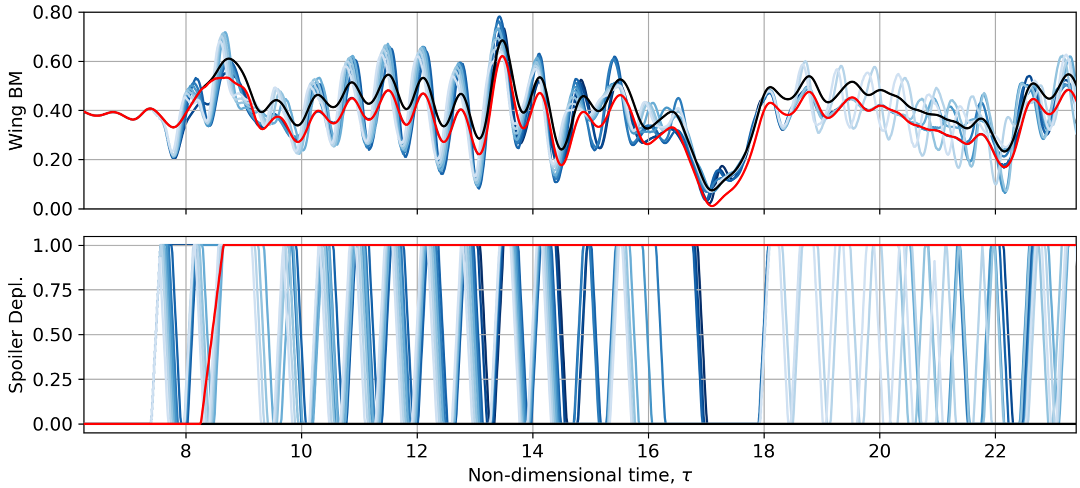

(b) Wing root bending moment and spoiler deflection time histories for a continuos turbulence gust

Figure 4: SMS dynamic response for different wing-tip displacement threshold retraction values (——: baseline model with no LAF; ——: actuated LAF; ——(from dark to light): SMS for different wing-tip displacement threshold retraction values)

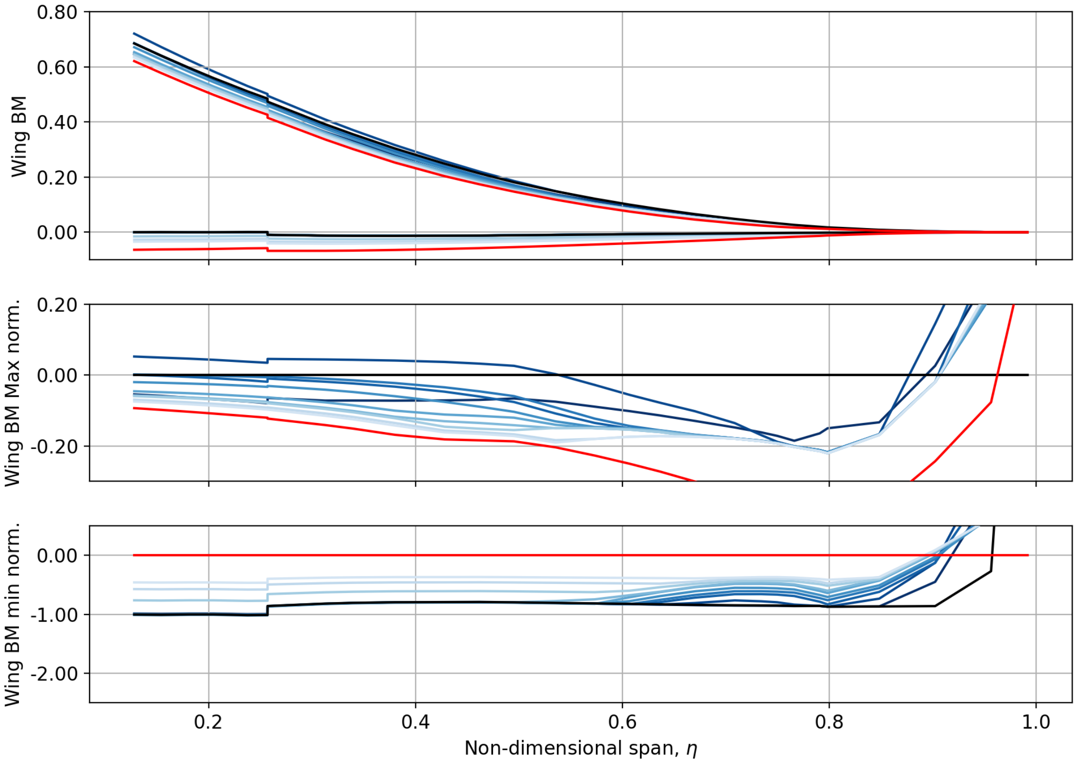

(a) Wing bending moment distribution - gust loads envelope

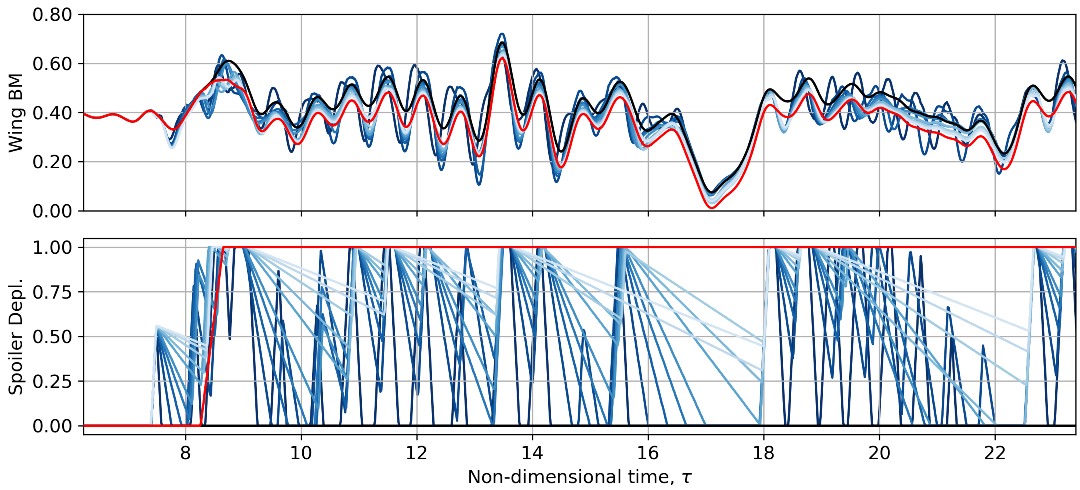

(b) Wing root bending moment and spoiler deflection time histories for a continuos turbulence gust

Figure 5: SMS dynamic response for different retraction speeds
(——: baseline model with no LAF; ——: actuated LAF;
——(from dark to light): SMS for different retraction speeds)